Obesity-Associated Hepatosteatosis and Impairment of Glucose Homeostasis Are Attenuated by Haptoglobin Deficiency

Simonetta Lisi,[1,2] Olimpia Gamucci,[2] Teresa Vottari,[1,2] Gaia Scabia,[1,2] Marcella Funicello,[1,2] Matilde Marchi,[1,2] Giulia Galli,[2] Ivan Arisi,[3] Rossella Brandi,[3] Mara D'Onofrio,[3] Aldo Pinchera,[2] Ferruccio Santini,[2] and Margherita Maffei[1,2]

OBJECTIVE—Haptoglobin (Hp) is upregulated in both inflammation and obesity. The low chronic inflammatory state, caused by massive adipose tissue macrophage (ATM) infiltration found in obesity, and low adiponectin have been implicated in the development of insulin resistance and hepatosteatosis. The aim of this work was to investigate whether and how Hp interferes with the onset of obesity-associated complications.

RESEARCH DESIGN AND METHODS—Hp-null ($Hp^{-/-}$) and wild-type (WT) mice were metabolically profiled under chow-food diet (CFD) and high-fat diet (HFD) feeding by assessing physical parameters, glucose tolerance, insulin sensitivity, insulin response to glucose load, liver triglyceride content, plasma levels of leptin, insulin, glucose, and adiponectin. ATM content was evaluated by using immunohistochemistry (anti-F4/80 antibody). Adiponectin expression was measured in Hp-treated, cultured 3T3-L1 and human adipocytes.

RESULTS—No genotype-related difference was found in CFD animals. HFD-$Hp^{-/-}$ mice revealed significantly higher glucose tolerance, insulin sensitivity, glucose-stimulated insulin secretion, and adiponectin expression and reduced hepatomegaly/steatosis compared with HFD-WT mice. White adipose tissue (WAT) of HFD-$Hp^{-/-}$ mice showed higher activation of insulin signaling cascade, lower ATM, and higher adiponectin expression. Hp was able to inhibit adiponectin expression in cultured adipocytes.

CONCLUSIONS—We demonstrated that in the absence of Hp, obesity-associated insulin resistance and hepatosteatosis are attenuated, which is associated with reduced ATM content, increased plasma adiponectin, and higher WAT insulin sensitivity.
Diabetes **60:2496–2505, 2011**

Haptoglobin (Hp) is a circulating tetrameric glycoprotein and is considered a classic clinical marker of the liver acute phase response to inflammation. Diversified functions have been attributed to this circulating protein, including angiogenic capacity, the ability to bind free hemoglobin, and, as recently demonstrated by the authors, an important chemotactic activity for monocytes in vitro (1–3). Hp is also abundantly expressed by white adipose tissue (WAT) (4,5), which is one of those few inflammatory molecules specifically produced by the adipocyte and not present in the stromal vascular fraction (6,7). Obesity has been recently defined as a low chronic inflammatory state, and this has been implicated in the development of common medically important complications, including hepatic steatosis, insulin resistance, and atherosclerosis (8–10). Classic markers of the obesity-induced inflammatory state include the augmented circulating levels of proinflammatory proteins, procoagulant factors, cytokines, and chemokines. The molecular and cytologic alterations taking place in WAT on obesity play a determinant role in this phenomenon. Obesity is in fact associated with increased infiltration of macrophages in WAT, and this certainly contributes to the inflammatory-like gene expression pattern displayed by the WAT of obese individuals. The mechanisms underlying macrophages recruitment are still a matter of investigation and likely involve increased secretion of chemotactic molecules by the adipocytes. Monocyte chemoattractant protein 1 (MCP-1) and its receptor C-C chemokine receptor 2 (CCR2) have been considered the main players in this process (11,12). Recent work by the authors demonstrates that Hp induces CCR2 internalization and that pharmacologic inhibition of CCR2 abolishes monocytes migration toward Hp (2).

As we previously reported, WAT Hp expression is induced in obesity and the circulating levels of the glycoprotein are significantly related to the degree of adiposity in humans (4,5). The depicted scenario thus far led to the consideration of Hp as a novel adipokine (5) and a further intersection between obesity and inflammation. However, if its role in the latter condition has long been established and characterized, its role in metabolism and WAT has yet to be fully elucidated.

In the current study, we investigated how variations in Hp expression might be relevant to metabolism and to WAT expression and inflammatory profile. These issues were investigated in mice by using the Hp-null ($Hp^{-/-}$) model, for which no metabolic characterization had been carried out (13). Our findings indicate that on the onset of obesity, Hp deficiency confers a partial protection against impaired glucose homeostasis and hepatomegaly/steatosis and that these features are associated with increased adiponectin and reduced WAT macrophage infiltration.

RESEARCH DESIGN AND METHODS

Experimental animals. $Hp^{-/-}$ mice were generated previously (13). Mice were fed a chow-food diet (CFD) (2018 Teklad Global Diet; Harlan, Indianapolis, IN) or high-fat diet (HFD) (Diet F3282, 19% protein, 36% fat, and 35% carbohydrate [gram per weight]; Bio-Serve, Frenchtown, NJ) for 12 weeks (Supplementary Appendix A1). Serum, epididymal (EPI) WAT, subcutaneous

From the [1]Dulbecco Telethon Institute, Rome, Italy; the [2]Department of Endocrinology and Kidney, University-Hospital of Pisa, Italy; and the [3]European Brain Research Institute, Rome, Italy.
Corresponding author: Margherita Maffei, mmaffei@dti.telethon.it, or Ferruccio Santini, ferruccio.santini@med.unipi.it.
Received 4 November 2010 and accepted 13 July 2011.
DOI: 10.2337/db10-1536
This article contains Supplementary Data online at http://diabetes.diabetesjournals.org/lookup/suppl/doi:10.2337/db10-1536/-/DC1.

(SC) WAT and perirenal fat pads, brown adipose tissue (BAT), kidney, and liver were dissected from fasted animals, weighed, and frozen in liquid nitrogen. Blood was withdrawn by cardiac puncture and from the tail vein (in live animals). The experimental protocols followed the Principles of Laboratory Animal Care and a specific authorization by the Italian Ministry of Education (114/2003-A of 16/09/2003) .

Ex vivo cultures and primary adipocytes. Tissue explants of visceral WAT, liver, and kidney from wild-type (WT) mice (5 months old, mean body weight [BW] 26.5 g) were isolated, cut into small pieces, and incubated in Dulbecco's modified Eagle's medium with antibiotics and 2% BSA at 37°C in 5% CO_2 atmosphere. Aliquots of the medium were taken at different time points. Hp concentration at time point 0 was considered as baseline and subtracted from values obtained afterward.

Primary adipocytes were prepared as described (14). After isolation, human adipocytes (Supplementary Appendix A2) were maintained in Dulbecco's modified Eagle's medium with 10% FBS, 100 units/mL penicillin, and 100 mg/mL streptomycin at 37°C with 5% CO_2. Cells were treated with human Hp (1 mg/mL) (Sigma-Aldrich, St. Louis, MO) for 24 h and collected at the end of treatment.

Culture and treatment of 3T3-L1. 3T3-L1 cells were differentiated in adipocytes as described previously (15). After differentiation, 3T3-L1 adipocytes were treated with BSA or Hp at different concentrations for 24 h and finally collected.

Isolation of total RNA and real-time PCR. Total RNA was isolated from frozen tissues (WAT, liver, and BAT) or from cells and retro-transcribed as described previously (14). TaqMan quantitative PCR was performed on an ABI-PRISM 7700 Sequence Detection System (Applied Biosystems, Carlsbad, CA) using Tata-binding protein as an endogenous control. Predesigned mouse primers and probes were obtained from Applied Biosystems.

Microarray analysis. The gene expression profiling was performed using the One-Color Microarray Agilent Platform (Agilent Technologies, Santa Clara, CA) according to the Agilent protocol (Agilent 8 × 60 K whole mouse genome oligonucleotide microarrays, G4852A) (Supplementary Appendix A3). Data extraction from the Agilent scanner images was accomplished by Feature Extraction software. Data filtering and analysis were performed using Agilent GeneSpring GX 11.0 and Microsoft Excel (Microsoft Corp., Redmond, WA). Filtered data were quantile-normalized. Differentially expressed genes were selected by Mann-Whitney *U* nonparametric test. Hierarchic clustering analysis was done using MeV 4.4 (16).

Glucose tolerance, insulin sensitivity, and ELISA. Glucose tolerance was measured in fasted (16 h) mice after intraperitoneal injection (intraperitoneal glucose tolerance test) of 1 g glucose/kg BW. Insulin sensitivity was measured in fasted (6 h) animals after intraperitoneal injection (intraperitoneal insulin tolerance test) of 1.2 units/kg insulin BW. Glucose-stimulated insulin secretion was performed as described by Nguyen et al. (17). Plasma glucose was measured using a glucometer (LifeScan, Inc., Milpitas, CA). ELISA kits were used to assess plasma levels of insulin (Millipore, Billerica, MA), leptin (R&D Systems, Inc., Minneapolis, MN), adiponectin, and Hp (R&D Systems, Inc.; Immunology Consultants Laboratory, Inc., Newberg, OR).

In vivo insulin signaling. Fasted mice (6 h) were injected with insulin (10 units/kg BW) and killed 10 min thereafter. Tissues were then promptly collected. After homogenization in ice-cold lysis buffer (Supplementary Appendix A4), lysates were centrifuged at 14,000*g* for 20 min at 4°C. Supernatants were resolved by SDS-PAGE (Criterion, Bio-Rad Laboratories, Hercules, CA). Phosphorylated and total proteins were identified by immunoblotting using the following primary antibodies: anti-Akt polyclonal and anti–phospho-Akt (Ser(P)473) (Cell Signaling Technology, Inc., Danvers, MA), and antiactin (Sigma-Aldrich). Immunoblots were developed using the Immun-Star HRP kit (Bio-Rad Laboratories), and densitometric analysis was performed using Quantity One software (Bio-Rad Laboratories).

Oil Red O staining and liver triglyceride content. To visualize the fat droplet accumulation, frozen liver tissue sections were stained with Oil Red O. To assess triglyceride content, liver samples were homogenized in 5% Triton X-100 in water. Samples were heated at 92°C for 5 min, cooled to room temperature, and spun at 14,000 rpm for 5 min at room temperature. Supernatants were used to assay triglyceride concentration using the Triglyceride Quantification Kit (Bio-Vision, Inc., Mountain View, CA).

Histology and immunohistochemistry. EPI, SC fat pads, and BAT were fixed in 10% formaldehyde and embedded in paraffin (Supplementary Appendix A5). BAT sections were stained with hematoxylin and eosin. EPI and SC (5-μm sections) were stained for F4/80 antibody (AbD Serotec, Kidlington, U.K.) and revealed by DAB (Vector Laboratories, Burlingame, CA), followed by counterstaining with hematoxylin.

Statistical analysis. All values are expressed as means ± SEM. Pairwise comparisons of quantitative phenotypes between different groups (e.g., HFD-WT vs. HFD-Hp$^{-/-}$) were assessed by two-tailed Student *t* test. When specified, one- or two-way ANOVA was used, followed by Bonferroni post hoc tests for selected comparisons.

RESULTS

Hp release by mouse WAT. According to Fain et al. (7), explants of human WAT release Hp into the medium. We wanted to verify whether mouse WAT displayed this same capacity. The release of Hp by EPI WAT explants was fairly linear over the incubation time (Fig. 1*A*). We then wanted to compare the release of Hp from WAT with that from liver, considered the main source for this glycoprotein (18), and from kidney, which conversely exhibits very low Hp expression (4). Over 24 h, liver was the greatest producer of Hp, and Hp production in WAT was significantly higher than in kidney (Fig. 1*B*). These results rule out the possibility that what was detected in the medium was due to the spillover of Hp contained in excised vessels, because a comparable amount of released Hp would be expected from all examined tissues. On the basis of these data, we calculated that the average daily release of Hp from visceral WAT and liver is 256 ± 92 and 660 ± 88 ng/g tissue per day, respectively. By taking into account that visceral WAT represents ~13% of the BW of an animal (the average BW of these animals is 26.5 g) and that the average liver weight is 1.5 g, the total Hp daily production can be estimated to attain 0.88 μg for visceral WAT and 0.99 μg for liver. Such an estimate for WAT contribution to circulating Hp is in the lower range, not including the Hp production by SC WAT.

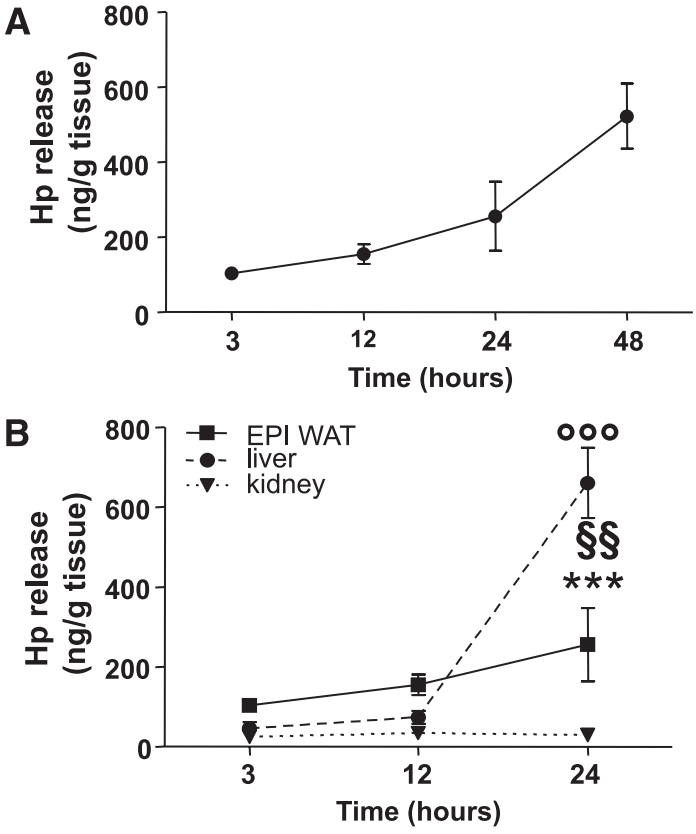

FIG. 1. Hp release into the medium by mouse tissue explants. *A*: Hp release from mouse EPI WAT is shown at 3, 12, 24, and 48 h. One-way ANOVA: $P < 0.01$. *B*: Hp release from mouse liver (circle), EPI WAT (square), and kidney (triangle) is shown at 3, 12, and 24 h. Two-way ANOVA: time effect $P < 0.0001$, tissue effect $P < 0.0001$, interaction $P < 0.0001$. Bonferroni post hoc tests at 24 h: EPI WAT vs. liver ***$P < 0.001$; EPI WAT vs. kidney §§$P < 0.01$, liver vs. kidney °°°$P < 0.001$. Data are expressed as means ± SEM of five experiments.

To rule out the possibility that the Hp release measured in mouse WAT explants was due to other cell types or to continuous and progressive spill-over from vessels trapped in the tissue, Hp concentration was assessed in the medium where primary mouse adipocytes had been cultured for 6 h. Hp was present in this medium at a concentration of 22.2 ± 1.9 ng/mL/10^6 cells. Although this value cannot be easily transformed into Hp release per gram of tissue, because a variable number of cells are lost during cell isolation and preparation, this result definitely establishes that adipocytes themselves are able to release Hp.

HFD results in increased Hp production in mice. We previously demonstrated that serum Hp is directly related to adiposity in humans (5). To investigate this aspect in mice, a group of WT mice was exposed to an HFD on which animals gained ~88% of their initial BW. Serum Hp was then assessed before and after HFD treatment, and a significant increase of serum Hp of approximately threefold was observed (Fig. 2*A*). *Hp* gene expression, as assessed by real-time PCR, was significantly higher in the EPI WAT but not in the liver of obese mice compared with lean mice (Fig. 2*B* and *C*). Taken together, these results suggest that in murine obesity *Hp* gene expression is specifically induced in WAT.

Physical parameters and plasma biochemistry of $Hp^{-/-}$ mice. To investigate the role of Hp in metabolism, an in vivo loss of function approach was undertaken. Adult $Hp^{-/-}$ mice and WT controls were analyzed under two different diet regimens, namely, CFD and HFD. HFD resulted in a significant increase in BW in both $Hp^{-/-}$ and WT animals compared with CFD-treated mice. No genotype effect was observed: WT and $Hp^{-/-}$ mice showed similar BW on a regular diet and did not differ in their susceptibility to gain weight when fed an HFD (Table 1). Weights of EPI and perirenal fat pads consistently were affected by diet but not by genotype (Fig. 3*A* and *B*). Likewise, BAT size was increased (independently of genotype) in HFD-treated mice (Fig. 3*C*). Histologic examination revealed that interscapular BAT of HFD-treated mice was composed mainly of hypertrophic unilocular cells as opposed to lean mice in which typical multilocular cells predominate (Fig. 3*D*), which is in line with other investigations (19–21). When concentrations of fasting glucose, insulin, and leptin were assessed, a diet effect was observed, but not a genotype effect (Table 1).

Hp deficiency results in ameliorated glucose homeostasis in obesity. Animals were challenged with an intraperitoneal glucose tolerance test. No genotype effect was observed in CFD-treated animals. (Fig. 4*A*). On HFD, WT mice exhibited an important glucose intolerance with no sign of glycemia decreasing at 120 min after glucose stimulus. This effect was attenuated in $Hp^{-/-}$ mice, for which a decrease, albeit moderate, was observed at 120 min. This is mirrored in the significantly lower value of the area under the curve exhibited by HFD-$Hp^{-/-}$ mice compared with WT mice (Fig. 4*B*). Of importance, HFD-$Hp^{-/-}$ mice displayed a clear glucose-stimulated insulin secretion, as opposed to WT mice, which showed no response (Fig. 4*C*).

During an intraperitoneal insulin tolerance test, HFD-$Hp^{-/-}$ mice were slightly more insulin-sensitive than HFD-WT mice (Fig. 4*D*). Of interest, an insulin-induced glucose decrease persisted for a longer period in the former.

Insulin action in liver, WAT, and skeletal muscle of HFD-$Hp^{-/-}$ mice. To better understand how global Hp deficiency contributes to define glucose homeostasis and

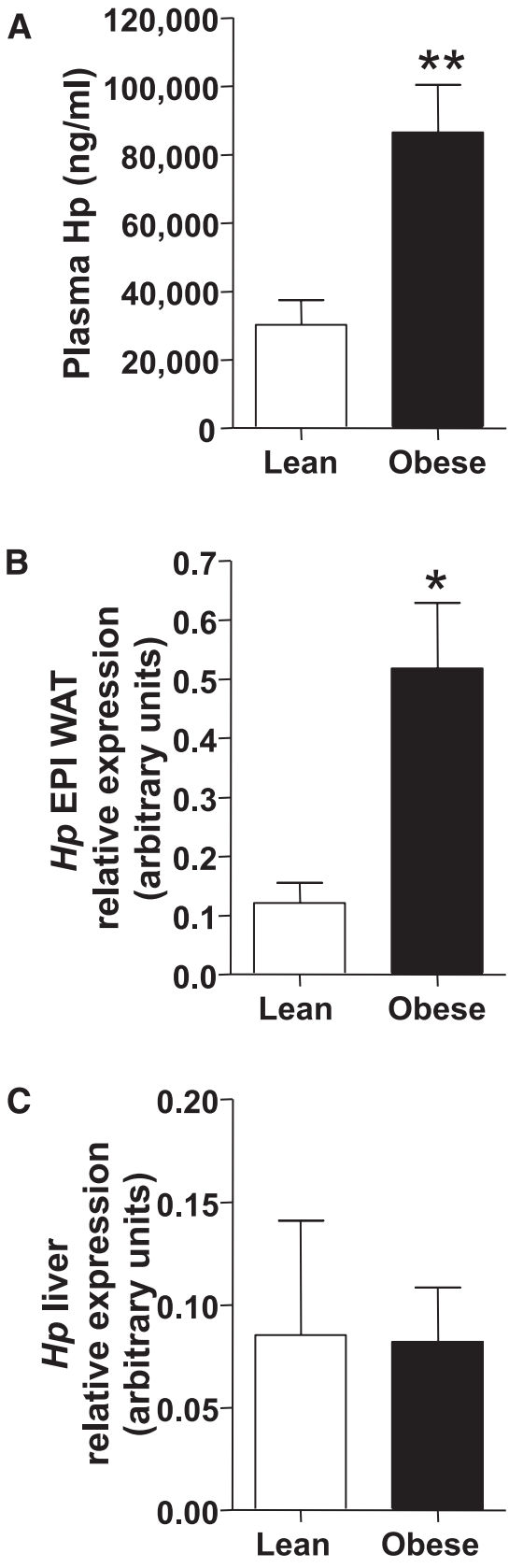

FIG. 2. HFD treatment results in increased Hp production. *A*: Hp plasma levels in lean (n = 7) and obese (n = 7) WT mice. *B*: *Hp* WAT mRNA abundance in lean and obese WT mice. *C*: *Hp* liver mRNA abundance in lean and obese WT mice. Student t test: *$P < 0.05$, **$P < 0.01$. Data are expressed as means ± SEM.

TABLE 1
Physical and metabolic parameters in WT and $Hp^{-/-}$ mice under CFD and HFD treatment

	CFD		HFD	
	WT (n = 15)	$Hp^{-/-}$ (n = 23)	WT (n = 24)	$Hp^{-/-}$ (n = 30)
Body weight (g)	27.36 ± 0.56	27.12 ± 0.30	42.29 ± 0.98	41.96 ± 0.54
Insulin (ng/mL)	0.88 ± 0.08	0.82 ± 0.09	2.35 ± 0.23	2.49 ± 0.26
Glucose (mg/dL)	148.78 ± 7.31	135.67 ± 8.02	235.23 ± 12.23	212.37 ± 7.02
Leptin (ng/mL)	2.8 ± 0.5	3.6 ± 0.9	74.1 ± 9.0*	89.7 ± 16.0†

Data are expressed as means ± SEM. Body weight: two-way ANOVA diet effect $P < 0.0001$. Insulin: two-way ANOVA diet effect $P < 0.0001$. Glucose: two-way ANOVA diet effect $P < 0.0001$. Leptin: two-way ANOVA diet effect $P < 0.0001$. *n = 18. †n = 22.

insulin sensitivity in HFD-treated mice, we evaluated insulin-stimulated phosphorylation of Akt Ser-473 in WAT, liver, and skeletal muscle (gastrocnemius). This was significantly enhanced in WAT and showed a trend toward increase in liver and skeletal muscle of HFD-$Hp^{-/-}$ mice compared with HFD-WT mice (Fig. 4*E*–*G*).

Taken together, these data suggest that Hp deficiency constitutes a partial protection against the onset of obesity-associated glucose intolerance, dampened glucose-stimulated insulin production, and insulin resistance. The latter is at least partially explained by a better preserved insulin response in the WAT.

Liver in lean and obese $Hp^{-/-}$ mice. Hp is abundantly expressed in the liver (18), and hepatosteatosis/hepatomegaly often characterizes obesity (22). Indeed, HFD-WT mice showed an important (35%) increase of their liver weight

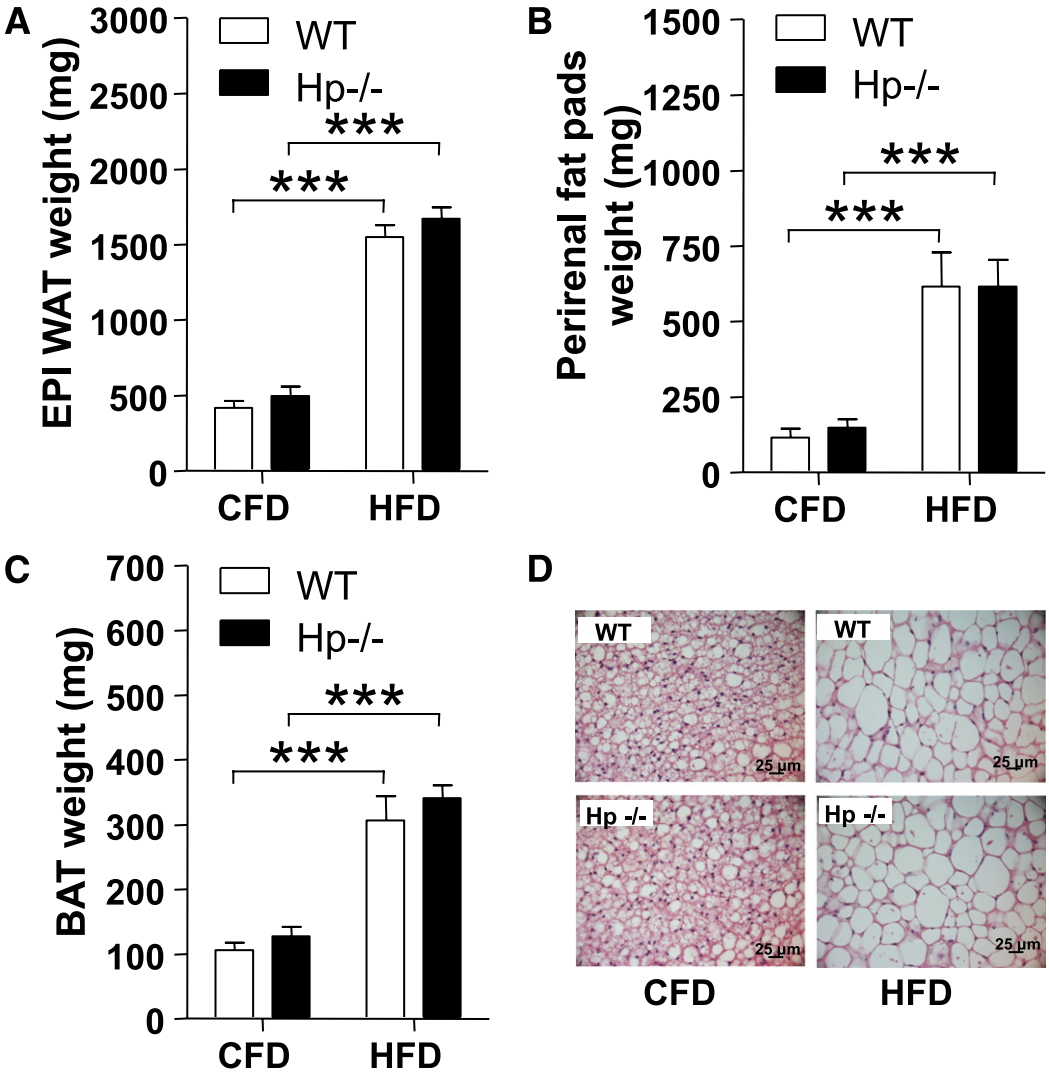

FIG. 3. HFD effects on adipose depots. Bar graphs showing weight of EPI WAT (*A*), perirenal fat pads (*B*), and BAT (*C*) in CFD- and HFD-WT and $Hp^{-/-}$ mice. Two-way ANOVA for *A*, *B*, *C*: diet effect $P < 0.0001$. Bonferroni post hoc test: CFD vs. HFD ***$P < 0.001$. Data are expressed as means ± SEM. *D*: Hematoxylin and eosin staining of 5-µm BAT sections of WT and $Hp^{-/-}$ mice under CFD or HFD treatment. (A high-quality color representation of this figure is available in the online issue.)

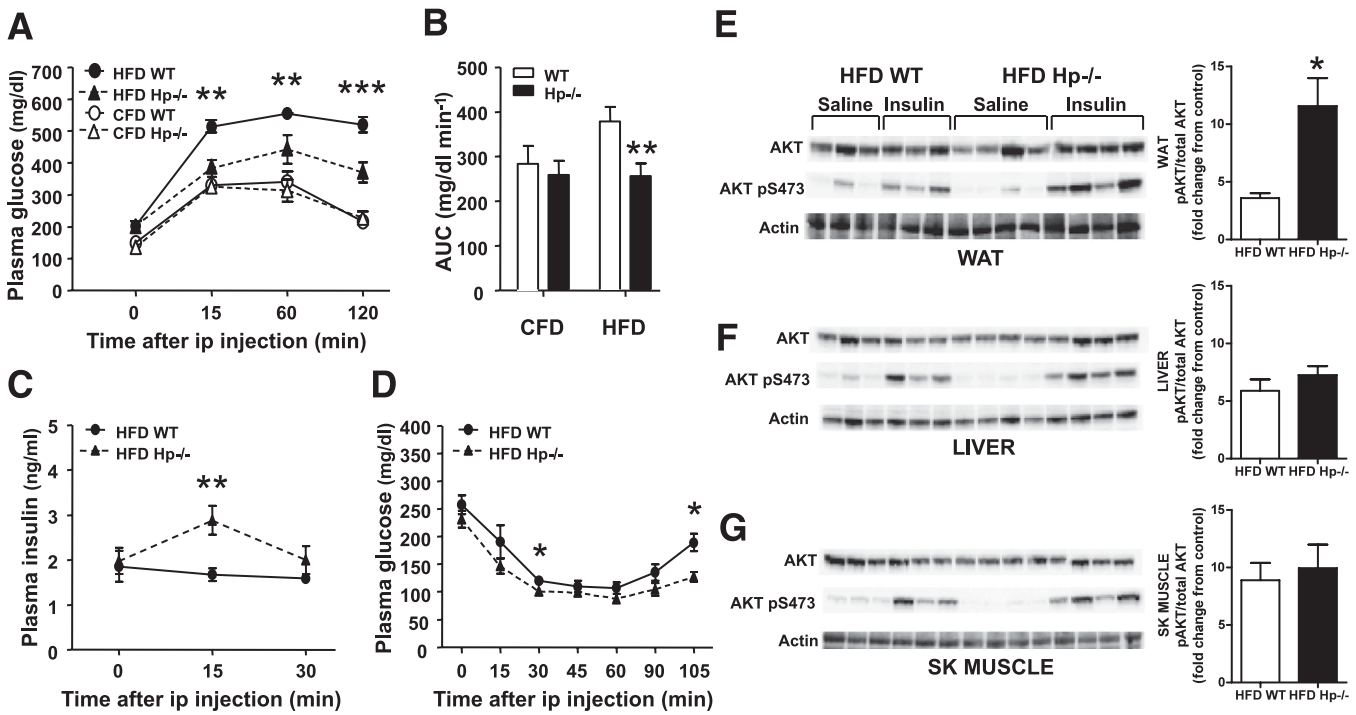

FIG. 4. Glucose homeostasis and insulin signaling of WT and Hp$^{-/-}$ mice. *A*: Intraperitoneal (ip) glucose tolerance test in CFD- and HFD-treated mice (n = 12). Two-way ANOVA: time effect, genotype effect, interaction $P < 0.0001$. Bonferroni post hoc tests: HFD-WT vs. HFD-Hp$^{-/-}$ **$P < 0.01$, ***$P < 0.001$. *B*: Area under the curve shown in *A*, calculated using the trapezoidal method. Student t test: HFD-WT vs. HFD-Hp$^{-/-}$ **$P < 0.01$. Data are expressed as means ± SEM. *C*: Glucose-stimulated insulin secretion in HFD-treated mice (n = 8). Two-way ANOVA: genotype effect $P < 0.01$. Bonferroni post hoc test at 15 min: HFD-WT vs. HFD-Hp$^{-/-}$ **$P < 0.01$. Data are expressed as means ± SEM. *D*: Intraperitoneal insulin tolerance test in HFD-treated mice (n = 8). Two-way ANOVA: time effect, genotype effect, $P < 0.0001$. Bonferroni post hoc test at 30 and 105 min: HFD-WT vs. HFD-Hp$^{-/-}$ *$P < 0.05$. Data are expressed as means ± SEM. *E–G*: Insulin signaling in vivo in WAT (*E*), liver (*F*), and skeletal muscle (*G*) of HFD-WT and HFD-Hp$^{-/-}$ mice. Mice (n = 3–4 per group) were fasted for 6 h, injected intraperitoneally with saline or insulin at 10 units/kg BW, and killed 10 min thereafter. Insulin-stimulated Ser473 phosphorylation of Akt was assessed by immunoblotting (*left*). Actin served as loading control. Quantification of phosphoproteins is shown in the corresponding bar graphs (*right*). Phosphoproteins were normalized to the corresponding total proteins and are expressed as fold changes from relative saline-treated control . Student t test: HFD-WT vs. HFD-Hp$^{-/-}$ *$P < 0.05$. Data are expressed as means ± SEM. AUC, area under the curve; SK, skeletal.

compared with CFD-WT mice. HFD treatment resulted in a less pronounced (15%, not significant) liver weight increase in Hp$^{-/-}$ mice (Fig. 5*A*).

Histological analysis revealed a lower lipid accumulation in the liver of Hp$^{-/-}$ mice (Fig. 5*B*). In line with this, triglyceride content was significantly lower in HFD-Hp$^{-/-}$ mice compared with HFD-WT mice (Fig. 5*C* and *D*).

To investigate the mechanisms underlying the reduced triglyceride accumulation observed in the liver of obese Hp$^{-/-}$ mice, we measured the abundance of transcripts for *1*) genes involved in lipid biosynthesis and metabolism, including the enzyme fatty acid synthase (*FAS*), the transcription factor sterol regulatory element-binding protein (*SREBP*), and the mitochondrial negative regulator of fatty acids oxidation glycerol 3-phosphate acyltransferase (*mtGPAT*); and *2*) two gluconeogenesis rate-limiting enzymes, namely, *PEPCK* and glucose-6 phosphatase (*G6Pase*). *FAS*, *SREBP*, *mtGPAT*, *PEPCK*, and *G6Pase* were downregulated by 66, 13, 53, 32, and 38%, respectively, in the liver of HFD-Hp$^{-/-}$ mice (Fig. 5*E*) compared with HFD-WT mice, which is consistent with decreased lipid synthesis, increased fatty acids β oxidation (23), and diminished gluconeogenesis (24).

Microarray analysis was used to better define the expression profile of HFD-Hp$^{-/-}$ versus HFD-WT mice. Hierarchical clustering identified WT and Hp$^{-/-}$ as two distinct groups. A total of 611 genes were differentially expressed, of which 573 were upregulated and 38 were downregulated in the HFD-Hp$^{-/-}$ (Fig. 5*F*). Among them, we chose to present those (Fig. 5*F*, right; Supplementary Appendix A6) more specifically related to liver functions/pathology and displaying more than a twofold change. Real-time PCR performed on two representative genes (cell death-inducing DNA fragmentation effector α [*CIDE*α] and acetyl-CoA carboxylase β [*ACAC*β]) confirmed microarray results (Supplementary Appendix A7).

If we exclude renin, glutathione *S*-transferases, and cytochrome P450 *CYP41*, the other nine genes could be placed in three functional categories, including *1*) apoptosis-related genes that include members of the serpin family (upregulated in HFD-Hp$^{-/-}$) and members of the *CIDE* family (downregulated in HFD-Hp$^{-/-}$), the former being inhibitors and the latter inducers of apoptosis; *2*) genes implied in lipid metabolism (downregulated in HFD-Hp$^{-/-}$); and *3*) transcription factors Forkhead box A2 (*FOXA2*) and hepatocyte nuclear factor 6 (*HNF6*), both associated with improved insulin sensitivity (25,26) when overexpressed and both upregulated in the absence of Hp (A6).

Adiponectin is increased in HFD-Hp$^{-/-}$ mice. Absence of Hp results in a more benign prognosis on the onset of obesity, because hepatomegaly/steatosis and insulin resistance are attenuated. For further insights into this matter, we searched for systemic or local factors that might explain such phenotype.

Adiponectin is a key factor in determining insulin sensitivity (27) because its plasma levels are inversely associated with glucose intolerance (28,29). Further, recent studies reported that hypoadiponectinemia enhances and

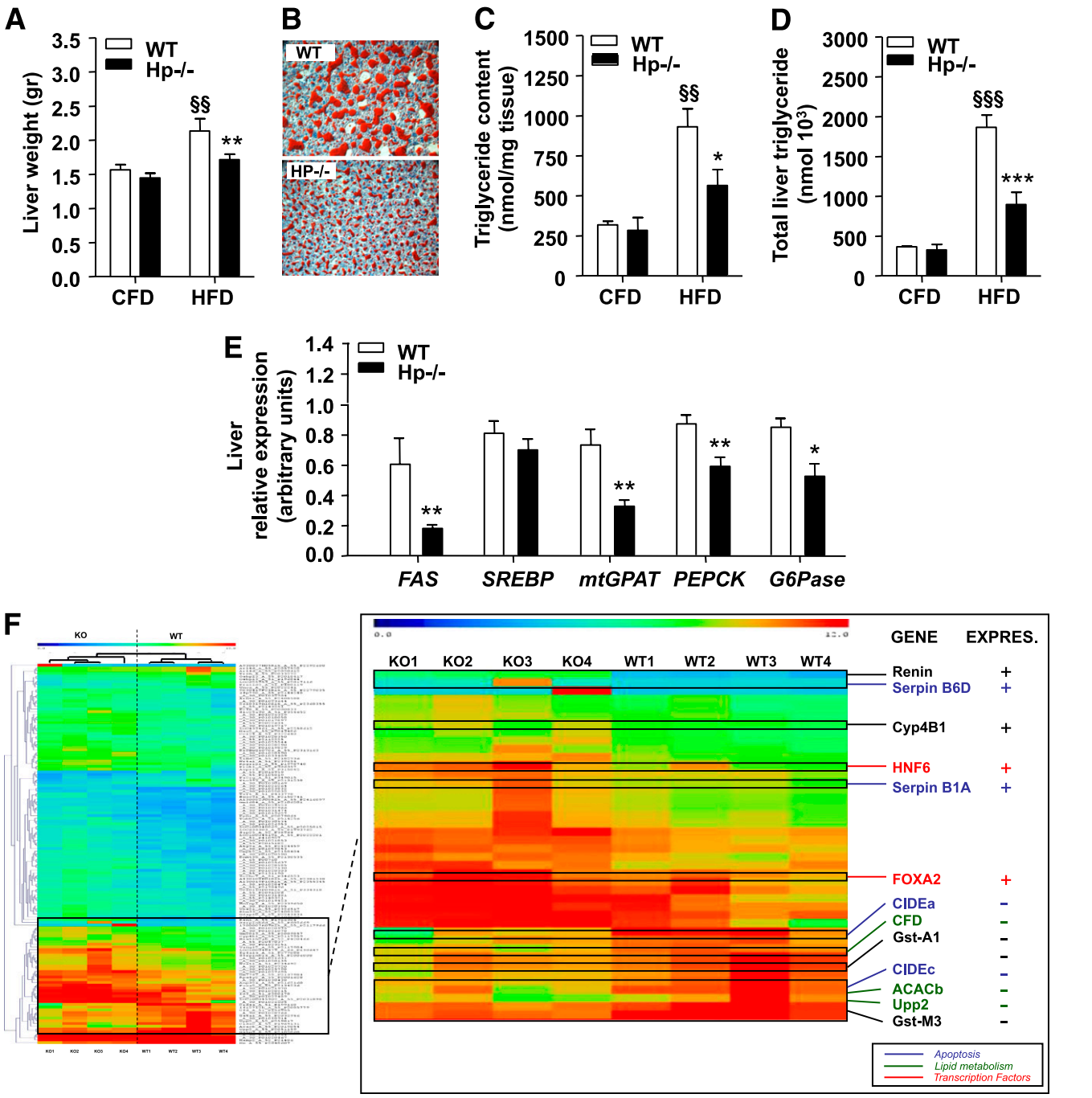

FIG. 5. Weight, triglyceride content, and gene expression in the liver of Hp$^{-/-}$ mice. *A*: Liver weight of WT and Hp$^{-/-}$ mice after CFD or HFD (n = 15). Two-way ANOVA: diet effect $P < 0.001$, genotype effect $P < 0.05$. *B*: Oil Red O staining of liver sections (8 μm) from HFD-WT and HFD-Hp$^{-/-}$ mice. *C*: Liver triglyceride content expressed per milligram of tissue. Two-way ANOVA: diet effect $P < 0.01$, genotype effect $P < 0.05$. *D*: Total liver triglyceride content in WT and Hp$^{-/-}$ mice. Two-way ANOVA: diet effect $P < 0.0001$, genotype effect $P < 0.01$, interaction $P < 0.05$. Bonferroni post hoc tests referred to *A*, *C*, and *D*: HFD-WT vs. HFD-Hp$^{-/-}$ *$P < 0.05$, **$P < 0.01$, ***$P < 0.001$. Bonferroni post hoc test CFD-WT vs. HFD-WT §§$P < 0.01$, §§§$P < 0.001$. Data are expressed as means ± SEM. *E*: Relative expression of genes involved in liver metabolism (*FAS*, *SREBP*, *mtGPAT*, *PEPCK*, and *G6Pase*) in HFD-WT and Hp$^{-/-}$ mice (n = 8). Student t test: HFD-WT vs. HFD-Hp$^{-/-}$ *$P < 0.05$, **$P < 0.01$. Data are expressed as means ± SEM. *F*: Microarray analysis of hepatic mRNA expression in HFD-WT and HFD-Hp$^{-/-}$ mice (n = 4). *Left*: Hierarchic clustering of 611 genes differentially expressed in the two genotypes. *Right*: Magnification showing 13 selected genes (see text). Nine of them were grouped in functional categories according to their biological function: apoptosis (in blue), transcription factors (in red), and lipid metabolism (in green). (A high-quality digital representation of this figure is available in the online issue.)

adiponectin administration prevents steatohepatitis progression in mice (30). We investigated this parameter in our models. Although plasma adiponectin was similar in CFD-WT and CFD-Hp$^{-/-}$ mice, HFD-Hp$^{-/-}$ exhibited significantly higher levels of adiponectin compared with HFD-WT mice (Fig. 6*A*). We also observed a significant increase of EPI WAT adiponectin mRNA in HFD-Hp$^{-/-}$ versus HFD-Hp-WT mice (Fig. 6*B*).

Effect of Hp on adiponectin expression in vitro. To investigate whether Hp plays a direct role on adiponectin expression, we performed in vitro experiments using 3T3-L1 adipocytes and purified Hp. Treatment of terminally

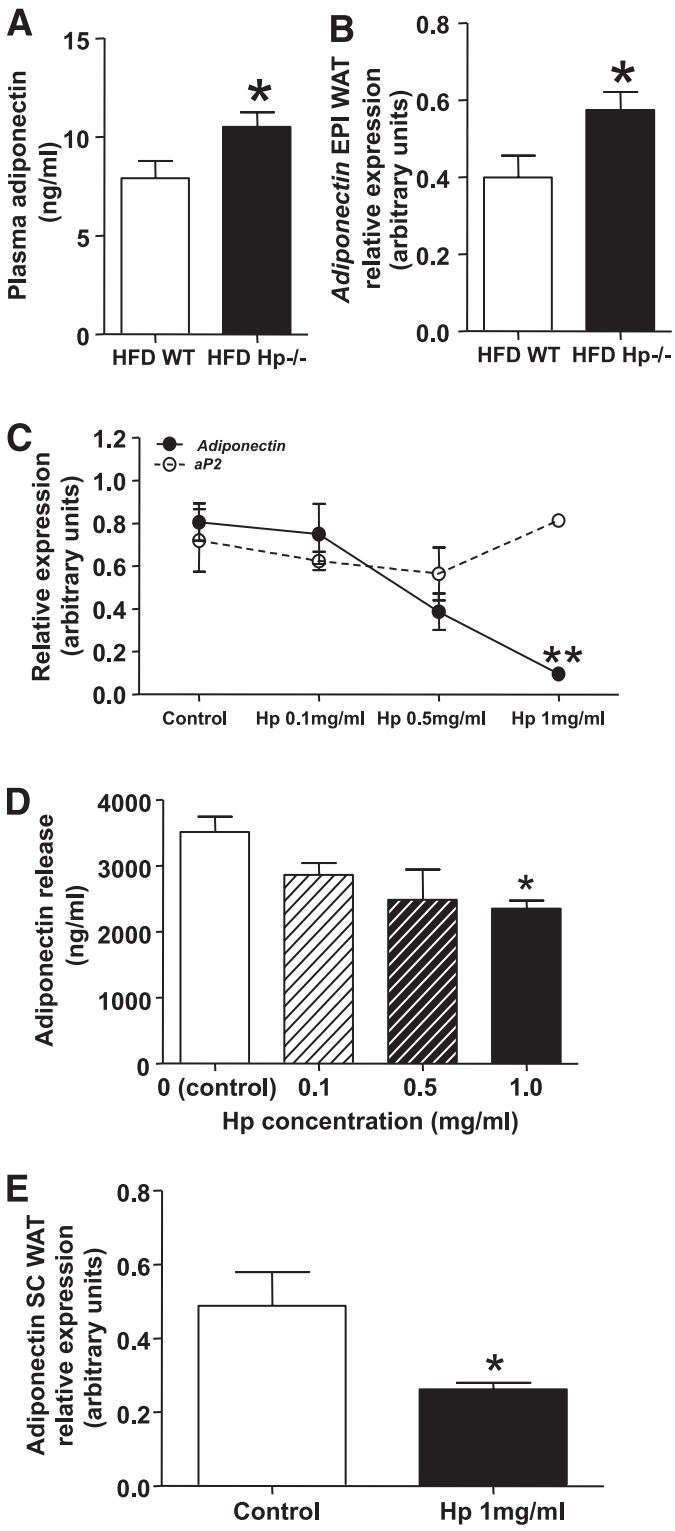

FIG. 6. Hp affects adiponectin expression in vivo and in vitro. *A*: Plasma adiponectin levels in HFD-WT and Hp$^{-/-}$ mice (n = 15). Student t test: *P < 0.05. *B*: Relative expression of adiponectin in EPI WAT of HFD-WT and Hp$^{-/-}$ mice. Student t test: *P < 0.05. *C*: Adiponectin and *aP2* relative gene expression in terminally differentiated 3T3-L1 adipocytes treated for 24 h with Hp as indicated. One-way ANOVA for adiponectin: P < 0.01. Bonferroni post hoc test: Hp 1 mg/mL vs. control **P < 0.01. *D*: Adiponectin release after Hp treatment for 24 h (doses as indicated) in terminally differentiated 3T3-L1 adipocytes. One-way ANOVA: P < 0.05. Bonferroni post hoc test: Hp 1 mg/mL vs. control *P < 0.05. *E*: Relative expression of adiponectin in SC human adipocytes, treated or not (control) with Hp for 24 h. Student t test: *P < 0.05. Data are expressed as means ± SEM.

differentiated adipocytes with Hp at different concentrations (0.1, 0.5, and 1 mg/mL) for 24 h resulted in a dose-dependent decrease of adiponectin mRNA compared with control cells treated with BSA (Fig. 6*C*). To rule out the possibility that Hp was exerting an aspecific effect on the adipocyte expression profile, we assessed the abundance of adipose fatty acid-binding protein-4 (*aP2*) mRNA in the same samples. No relevant change was determined. Hp effects on adiponectin mRNA abundance were paralleled by effects on adiponectin protein concentration in the medium. After 24 h of treatment, Hp induced a significant dose-dependent decrease of adiponectin (Fig. 6*D*). Of note, a downregulation of adiponectin mRNA abundance was observed also in primary human adipocytes treated with Hp (Fig. 6*E*). Taken together, these data indicate that Hp inhibits adiponectin expression in vitro.

WAT macrophage content in Hp$^{-/-}$ mice. Another important determinant of the risk to develop obesity-associated complications resides in the WAT inflammatory status. Having previously proved that Hp acts as a chemoattractant in vitro (2) and that it is released by murine WAT (present study), we wanted to establish whether a deficiency of this glycoprotein could affect WAT macrophage infiltration in vivo.

When HFD-treated mice were considered, a significantly lower macrophage infiltration was found in both EPI and SC WAT of Hp$^{-/-}$ compared with WT, as assessed by macrophage-specific surface protein F4/80 immunoreactivity (Fig. 7*A* and *B*). The abundance of macrophage-specific mRNAs (*F4/80* and *CD68*) consistently was lower in EPI WAT of obese Hp$^{-/-}$ mice compared with weight-matched WT mice (Fig. 7*C*). No genotype-related difference was observed in the ATM content of CFD-treated mice (data not shown).

These results are consistent with a role of Hp in contributing to WAT macrophage infiltration and consequent onset of altered inflammatory status at this site.

DISCUSSION

Inflammation/obesity is becoming an inseparable binomial association that has yet to be fully unraveled in terms of clinical consequences and underlying cytologic, biochemical, and molecular mechanisms. Hp, an inflammatory molecule that is upregulated in the WAT of obese subjects, constitutes an interesting tool to further explore this relationship.

We demonstrated that murine WAT not only expresses but also releases Hp at levels that equal, if not overcome, the hepatic release in terms of contribution to Hp-circulating concentration. We also prove that in obese mice, which show increased serum Hp, WAT *Hp* expression is increased, but not liver *Hp* expression, suggesting that obesity induces a specific WAT Hp upregulation. These premises should be considered in the context of the better preservation of glucose homeostasis shown by the Hp-deficient model of obesity. The concept of WAT being relevant for this phenotype is reinforced by insulin signaling studies that indicate this organ as the one with the highest increase (with respect to HFD-WT mice) in insulin sensitivity, among metabolically active tissues.

Lack of Hp attenuates the hepatomegaly/steatosis often associated with the obesity state. In addition to less-activated machinery for triglyceride accumulation, microarray analysis showed changes in HFD-Hp$^{-/-}$ liver expression profile that are consistent with lower activation of the apoptotic pathways. Apoptosis is a classic feature of hepatic steatosis progressing toward hepatitis and irreversible liver damage (31,32), and what we observe on Hp deficiency is, therefore,

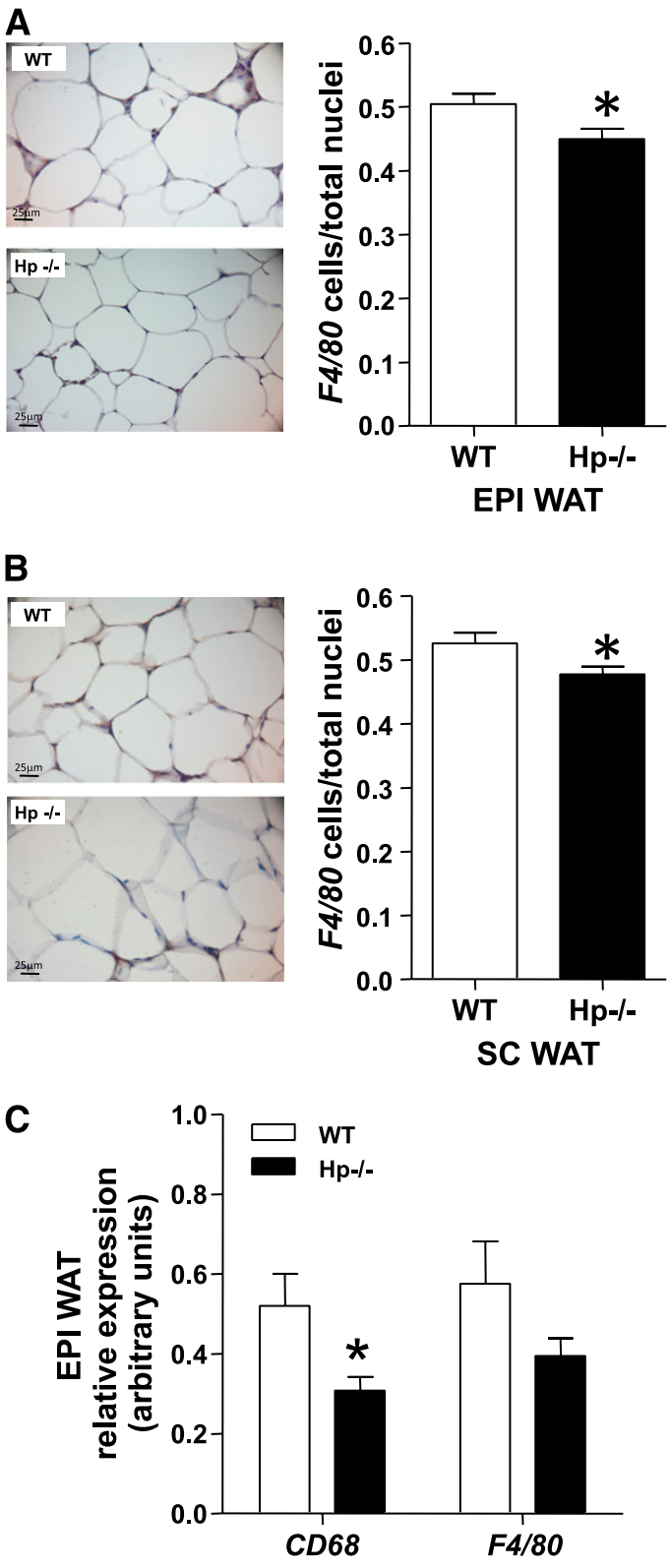

FIG. 7. ATM content in HFD-Hp$^{-/-}$ mice. *Left*: Immunohistochemical detection of F4/80 in EPI WAT (*A*) and SC WAT (*B*) of HFD-WT and Hp$^{-/-}$ mice. *Right*: Bar graphs indicating F4/80 stained cells/total nuclei in EPI WAT (*A*) (n = 7, 15 fields per animal) and SC WAT (*B*) (n = 8, 15 fields per animal). F4/80 positive macrophages from each individual depot were counted using a 40× objective. The ratio of F4/80-positive cells was calculated as the number of F4/80 positive nuclei divided by the total number of nuclei in the same field. *C*: EPI WAT gene expression of *CD68* and *F4/80* in HFD-WT and Hp$^{-/-}$ mice. Student t test: *P < 0.05. Data are expressed as means ± SEM. (A high-quality color representation of this figure is available in the online issue.)

consistent with a phenotype that is more protected against this risk. Whether such changes in liver expression are the result of local, systemic, or both Hp actions cannot be established on the basis of the present findings. The local scenario implies an Hp autocrine effect, possibly modulating deleterious gene expression programs. According to the systemic hypothesis, the liver is healthier because of surrounding conditions of improved glucose homeostasis and insulin sensitivity, determined by other organs.

In this regard, benign consequences of Hp deficiency are associated with reduced WAT macrophage infiltration and higher adiponectin levels. Both aspects imply a direct involvement of WAT, which is in line with the specific WAT Hp upregulation induced by obesity in the WT mouse. WAT dysfunction was previously associated with hepatosteatosis, and plasma Hp was defined as a prognostic marker for nonalcoholic steatohepatitis in animals exposed to HFD (33).

We recently reported that Hp is a chemotactic molecule (2), which is consistent with the reduced ATM infiltration observed in the obese Hp$^{-/-}$ mice. Macrophage infiltration in the WAT of obese individuals is related to the low chronic inflammatory state that often characterizes the obesity status. In particular, the release of inflammatory factors by macrophages, such as interleukin-6 and tumor necrosis factor-α, contributes to the onset of insulin resistance (34). Hepatic steatosis is also generally associated with the inflamed WAT: Mechanisms postulated to explain this association include a secondary effect of the altered availability of lipids generated by the insulin resistance state and a direct consequence of the altered WAT expression profile (35). As previously reported, increased fat content in the liver is independent of the degree of obesity (36) but significantly associated with WAT inflammation, and specifically with the abundance of inflammatory markers, including CD68 and MCP-1. MCP-1 was initially described as a potent chemoattractant factor (37) implicated in the recruitment of macrophages in WAT. Supporting evidence in this direction derives from the increased infiltration of macrophages observed in lean mice overexpressing MCP-1 in WAT (11) and consistently from the lower ATM content found in obese mice deficient for this factor (11) or for its receptor (CCR2) (12). In contrast, Inouye et al. (38) reported that macrophage content in the WAT of MCP-1 $^{-/-}$ obese mice is, if nothing, higher than that of obese controls. In no case did genetic obese models for MCP-1 or CCR2 exhibit a level of ATM normalized to that observed in lean mice, thus implying the presence of other uncovered factors in the modulation of this phenomenon. According to our previously published and currently reported evidence, Hp presents all of the features to be considered one of them. Tissue distribution differentiates MCP-1 from Hp, because abundance in WAT of the former is prevalently due (>80%) to its expression in the stromal vascular fraction (39), whereas Hp gene expression and release are almost totally confined to the adipocyte fraction (6). This strengthens the notion that the adipocyte itself is able to produce chemotactic molecules and attract macrophages both by active release and by simple spill-over in case of cell death (40). We previously demonstrated that Hp is able to internalize CCR2 in cultured monocytes and that pharmacologic inhibition of this chemokine receptor results in the abolition of Hp chemotactic activity (2), thus suggesting that Hp interacts with CCR2 to recruit macrophages. As we found for the obese Hp$^{-/-}$ mice, CCR2 $^{-/-}$ animals exposed to an HFD showed reduced ATM content, improved insulin

sensitivity, reduced hepatic steatosis, and increased adiponectin (12). Obese $Hp^{-/-}$ mice show higher adiponectin expression compared with controls. This adipokine is considered an important player in the determination of insulin sensitivity. A large amount of evidence points to the lack of a sufficient amount of this factor as a key signal for the onset of insulin resistance (41) and for the development of hepatic steatosis. In HFD-treated mice, decreased adiponectin often precedes steatohepatitis (42) and adiponectin reverses steatosis in *ob/ob* mice (43). Obese $Hp^{-/-}$ mice exhibit higher circulating and local levels of adiponectin compared with matched WT controls, which may partly explain their improved glucose tolerance and reduced hepatosteatosis. Our observation regarding adiponectin in HFD-treated $Hp^{-/-}$ mice was independently proved by the inhibitory effect exerted by Hp on adiponectin expression and secretion in cultured adipocytes. To our knowledge, this is the first report demonstrating that adiponectin is significantly downregulated by Hp, thus introducing a new player in the regulation of this adipokine. Accordingly, similar inhibitory capacities were previously reported for other inflammatory factors, including tumor necrosis factor-α and interleukin-6 (44–47), also upregulated in the WAT of obese subjects.

In conclusion, we have established that Hp not only marks the intersection between obesity and inflammation but also actively contributes to the WAT inflammatory profile often found in obese subjects and to the downregulation of adiponectin. These features may explain the phenotype of the obese $Hp^{-/-}$ mouse that is partially protected from the onset of obesity-associated complications, including severe insulin resistance and hepatosteatosis/hepatomegaly.

ACKNOWLEDGMENTS

S.L., T.V., G.S., M.F., and M.Mar. are supported by a Telethon fellowship. M.Maf. is an Associate Telethon Scientist. This work was supported by the Telethon Foundation (TCP99016), by Compagnia di San Paolo, and by the Italian Ministry of University and Research (Prot. 2008 3ZAXYC_004 to F.S.).

No potential conflicts of interest relevant to this article were reported.

S.L. researched data, analyzed data, and wrote the manuscript. O.G. and G.S. researched and analyzed data. T.V., M.F., M.Mar., and G.G. researched data. I.A. and R.B. performed microarray experiments. M.D. analyzed microrray data and contributed to discussion. A.P. contributed to discussion. F.S. contributed to experimental design and discussion. M.Maf. designed the experiments, analyzed data, and wrote the manuscript. All authors reviewed and edited the manuscript.

The authors thank Dr. Antonino Cattaneo (European Brain Research Institute, Rome) for supervision and support during microarray studies and Dr. Franklin G. Berger (University of South Carolina) for providing founders of the $Hp^{-/-}$ mouse colony.

REFERENCES

1. Cid MC, Grant DS, Hoffman GS, Auerbach R, Fauci AS, Kleinman HK. Identification of haptoglobin as an angiogenic factor in sera from patients with systemic vasculitis. J Clin Invest 1993;91:977–985
2. Maffei M, Funicello M, Vottari T, et al. The obesity and inflammatory marker haptoglobin attracts monocytes via interaction with chemokine (C-C motif) receptor 2 (CCR2). BMC Biol 2009;7:87
3. McCormick DJ, Atassi MZ. Hemoglobin binding with haptoglobin: delineation of the haptoglobin binding site on the alpha-chain of human hemoglobin. J Protein Chem 1990;9:735–742
4. Chiellini C, Bertacca A, Novelli SE, et al. Obesity modulates the expression of haptoglobin in the white adipose tissue via TNFalpha. J Cell Physiol 2002;190:251–258
5. Chiellini C, Santini F, Marsili A, et al. Serum haptoglobin: a novel marker of adiposity in humans. J Clin Endocrinol Metab 2004;89:2678–2683
6. do Nascimento CO, Hunter L, Trayhurn P. Regulation of haptoglobin gene expression in 3T3-L1 adipocytes by cytokines, catecholamines, and PPARgamma. Biochem Biophys Res Commun 2004;313:702–708
7. Fain JN, Madan AK, Hiler ML, Cheema P, Bahouth SW. Comparison of the release of adipokines by adipose tissue, adipose tissue matrix, and adipocytes from visceral and subcutaneous abdominal adipose tissues of obese humans. Endocrinology 2004;145:2273–2282
8. Berg AH, Scherer PE. Adipose tissue, inflammation, and cardiovascular disease. Circ Res 2005;96:939–949
9. Browning JD, Horton JD. Molecular mediators of hepatic steatosis and liver injury. J Clin Invest 2004;114:147–152
10. Lazar MA. How obesity causes diabetes: not a tall tale. Science 2005;307:373–375
11. Kanda H, Tateya S, Tamori Y, et al. MCP-1 contributes to macrophage infiltration into adipose tissue, insulin resistance, and hepatic steatosis in obesity. J Clin Invest 2006;116:1494–1505
12. Weisberg SP, Hunter D, Huber R, et al. CCR2 modulates inflammatory and metabolic effects of high-fat feeding. J Clin Invest 2006;116:115–124
13. Lim SK, Kim H, Lim SK, et al. Increased susceptibility in Hp knockout mice during acute hemolysis. Blood 1998;92:1870–1877
14. Funicello M, Novelli M, Ragni M, et al. Cathepsin K null mice show reduced adiposity during the rapid accumulation of fat stores. PLoS ONE 2007;2:e683
15. Maiuri T, Ho J, Stambolic V. Regulation of adipocyte differentiation by distinct subcellular pools of protein kinase B (PKB/Akt). J Biol Chem 2010;285:15038–15047
16. Saeed AI, Bhagabati NK, Braisted JC, et al. TM4 microarray software suite. Methods Enzymol 2006;411:134–193
17. Nguyen KT, Tajmir P, Lin CH, et al. Essential role of Pten in body size determination and pancreatic beta-cell homeostasis in vivo. Mol Cell Biol 2006;26:4511–4518
18. Bensi G, Raugei G, Klefenz H, Cortese R. Structure and expression of the human haptoglobin locus. EMBO J 1985;4:119–126
19. Cinti S, Frederich RC, Zingaretti MC, De Matteis R, Flier JS, Lowell BB. Immunohistochemical localization of leptin and uncoupling protein in white and brown adipose tissue. Endocrinology 1997;138:797–804
20. Ainslie DA, Proietto J, Fam BC, Thorburn AW. Short-term, high-fat diets lower circulating leptin concentrations in rats. Am J Clin Nutr 2000;71:438–442
21. Harada K, Shen WJ, Patel S, et al. Resistance to high-fat diet-induced obesity and altered expression of adipose-specific genes in HSL-deficient mice. Am J Physiol Endocrinol Metab 2003;285:E1182–E1195
22. Van Steenbergen W, Lanckmans S. Liver disturbances in obesity and diabetes mellitus. Int J Obes Relat Metab Disord 1995;19(Suppl. 3):S27–S36
23. Lindén D, William-Olsson L, Rhedin M, Asztély AK, Clapham JC, Schreyer S. Overexpression of mitochondrial GPAT in rat hepatocytes leads to decreased fatty acid oxidation and increased glycerolipid biosynthesis. J Lipid Res 2004;45:1279–1288
24. Samuel VT, Liu ZX, Qu X, et al. Mechanism of hepatic insulin resistance in non-alcoholic fatty liver disease. J Biol Chem 2004;279:32345–32353
25. Wolfrum C, Asilmaz E, Luca E, Friedman JM, Stoffel M. Foxa2 regulates lipid metabolism and ketogenesis in the liver during fasting and in diabetes. Nature 2004;432:1027–1032
26. Wang M, Chen M, Zheng G, et al. Transcriptional activation by growth hormone of HNF-6-regulated hepatic genes, a potential mechanism for improved liver repair during biliary injury in mice. Am J Physiol Gastrointest Liver Physiol 2008;295:G357–G366
27. Berg AH, Combs TP, Du X, Brownlee M, Scherer PE. The adipocyte-secreted protein Acrp30 enhances hepatic insulin action. Nat Med 2001;7:947–953
28. Ryan AS, Berman DM, Nicklas BJ, et al. Plasma adiponectin and leptin levels, body composition, and glucose utilization in adult women with wide ranges of age and obesity. Diabetes Care 2003;26:2383–2388
29. Winzer C, Wagner O, Festa A, et al. Plasma adiponectin, insulin sensitivity, and subclinical inflammation in women with prior gestational diabetes mellitus. Diabetes Care 2004;27:1721–1727
30. Fukushima J, Kamada Y, Matsumoto H, et al. Adiponectin prevents progression of steatohepatitis in mice by regulating oxidative stress and Kupffer cell phenotype polarization. Hepatol Res 2009;39:724–738
31. Malhi H, Guicciardi ME, Gores GJ. Hepatocyte death: a clear and present danger. Physiol Rev 2010;90:1165–1194
32. Yin XM, Ding WX. Death receptor activation-induced hepatocyte apoptosis and liver injury. Curr Mol Med 2003;3:491–508

33. Duval C, Thissen U, Keshtkar S, et al. Adipose tissue dysfunction signals progression of hepatic steatosis towards nonalcoholic steatohepatitis in C57BL/6 mice. Diabetes 2010;59:3181–3191. Epub 2010 Sep 21.
34. Bourlier V, Bouloumie A. Role of macrophage tissue infiltration in obesity and insulin resistance. Diabetes Metab 2009;35:251–260
35. Marra F, Bertolani C. Adipokines in liver diseases. Hepatology 2009;50: 957–969
36. Kolak M, Westerbacka J, Velagapudi VR, et al. Adipose tissue inflammation and increased ceramide content characterize subjects with high liver fat content independent of obesity. Diabetes 2007;56:1960–1968
37. Yoshimura T, Yuhki N, Moore SK, Appella E, Lerman MI, Leonard EJ. Human monocyte chemoattractant protein-1 (MCP-1). Full-length cDNA cloning, expression in mitogen-stimulated blood mononuclear leukocytes, and sequence similarity to mouse competence gene JE. FEBS Lett 1989;244:487–493
38. Inouye KE, Shi H, Howard JK, et al. Absence of CC chemokine ligand 2 does not limit obesity-associated infiltration of macrophages into adipose tissue. Diabetes 2007;56:2242–2250
39. Di Gregorio GB, Yao-Borengasser A, Rasouli N, et al. Expression of CD68 and macrophage chemoattractant protein-1 genes in human adipose and muscle tissues: association with cytokine expression, insulin resistance, and reduction by pioglitazone. Diabetes 2005;54:2305–2313
40. Cinti S, Mitchell G, Barbatelli G, et al. Adipocyte death defines macrophage localization and function in adipose tissue of obese mice and humans. J Lipid Res 2005;46:2347–2355
41. Cook JR, Semple RK. Hypoadiponectinemia—cause or consequence of human "insulin resistance"? J Clin Endocrinol Metab 2010;95:1544–1554
42. Larter CZ, Yeh MM, Van Rooyen DM, et al. Roles of adipose restriction and metabolic factors in progression of steatosis to steatohepatitis in obese, diabetic mice. J Gastroenterol Hepatol 2009;24:1658–1668
43. Xu A, Wang Y, Keshaw H, Xu LY, Lam KS, Cooper GJ. The fat-derived hormone adiponectin alleviates alcoholic and nonalcoholic fatty liver diseases in mice. J Clin Invest 2003;112:91–100
44. Fasshauer M, Kralisch S, Klier M, et al. Adiponectin gene expression and secretion is inhibited by interleukin-6 in 3T3-L1 adipocytes. Biochem Biophys Res Commun 2003;301:1045–1050
45. Hajer GR, van Haeften TW, Visseren FL. Adipose tissue dysfunction in obesity, diabetes, and vascular diseases. Eur Heart J 2008;29:2959–2971
46. Havel PJ. Update on adipocyte hormones: regulation of energy balance and carbohydrate/lipid metabolism. Diabetes 2004;53(Suppl. 1):S143–S151
47. Maeda N, Takahashi M, Funahashi T, et al. PPARgamma ligands increase expression and plasma concentrations of adiponectin, an adipose-derived protein. Diabetes 2001;50:2094–2099